Synthesis and X-ray Powder Structures of Nickel(II) and Copper(II) Coordination Polymers with 2,5-Bis(2-pyridyl)pyrazine

Antonia Neels, Bernard Mathez Neels, and Helen Stoeckli-Evans*

Institut de Chimie, Université de Neuchâtel, Avenue de Bellevaux 51, CH-2000 Neuchâtel, Switzerland

Abraham Clearfield and Damodara M. Poojary

Department of Chemistry, Texas A&M University, College Station, Texas 77843

Received February 14, 1997[⊗]

The reaction of 2,5-bis(2-pyridyl)pyrazine (bppz) with nickel(II) sulfate in aqueous solution yielded a binuclear complex, $[Ni_2(bppz)(H_2O)_8](SO_4)_2 \cdot 2H_2O$ **(1)**, whose structure was solved by single-crystal methods. The compound crystallizes in the monoclinic space group $P2_1/n$ with $a = 8.372(2)$ Å, $b = 18.301(2)$ Å, $c = 17.197(2)$ Å, $\beta = 97.54(2)°$, and $Z = 4$. The bppz ligand chelates the two octahedrally coordinated nickel atoms through its nitrogen donors. The four remaining coordination sites are occupied by water oxygen atoms. The binuclear $[Ni_2(bppz)(H_2O)_8]^{4+}$ cations are held together by hydrogen bonds involving sulfate anions and water molecules. Similar reactions with nickel(II) or copper(II) chloride in less polar solvents resulted in the formation of two new coordination polymers, $\{[Ni_2Cl_2(bppz)(H_2O)_2(CH_3OH)_2]Cl_2\}_n$ **(2)** and $[Cu_2Cl_4(bppz)]_n$ **(3)**. These polymers could be obtained only in microcrystalline form. Their structures were determined *ab initio* from X-ray powder diffraction data. The complex $\{[Ni_2Cl_2(bppz)(H_2O)_2(CH_3OH)_2]Cl_2\}_n$ **(2)** belongs to the triclinic space group $P\bar{1}$ with $a = 8.7014(4)$ Å, $b = 10.1465(5)$ Å, $c = 8.0303(3)$ Å, $\alpha = 116.095(2)°$, $\beta = 112.713(3)°$, $\gamma = 64.056(3)°$, and $Z = 1$. The octahedral coordination of the nickel atom is achieved by two nitrogens of the ligand bppz, two chloride ions, and two oxygens from the solvent molecules. The bridging nature of the chloride ions and the bis-bidentate ligands (bppz) leads to a one-dimensional polymer. The compound $[Cu_2Cl_4(bppz)]_n$ **(3)** crystallizes in the monoclinic space group $C2/m$ with $a = 13.9124(5)$ Å, $b = 6.1844(2)$ Å, $c = 10.1572(3)$ Å, $\beta = 112.952(3)°$, and $Z = 2$. The copper atoms display a distorted octahedral geometry where four of the coordination sites are occupied by chloride ions and the remaining two by nitrogen atoms of bppz. The metal atoms are bridged by two chlorine atoms and the bppz ligands, forming a two-dimensional coordination polymer.

Introduction

Coordination metal complexes with polymeric structures are of special interest in the development of new materials. Molecular-based ferromagnets, synthetic-metal conductors, nonlinear optical materials, and electronic materials are some of their important applications.[1] Coordination polymers can be prepared by the use of bridging polydentate ligands. 2,5-Bis-(2-pyridyl)pyrazine (bppz) is one such ligand, which we have used for the preparation of a number of polymeric structures.[2] This ligand also has the ability to form supra- or nanomolecular species, as was shown by Denti and co-workers.[3,4]

Using bppz, we[5] and others[6] have isolated binuclear complexes of the 3d series of transition metals. Such a reaction was favored in aqueous solution in the presence of oxygen-rich anions such as nitrates, sulfates, and hexafluoroacetylacetonates. These binuclear complexes could then be linked into polymeric species by the use of acetates or benzoates.[7,8] Magnetic measurements show antiferromagnetic properties for such coordination polymers. Interestingly, it is found that the metal atoms bridged by the bppz ligand show only a weak antiferromagnetic interaction while strong antiferromagnetic coupling is observed between copper atoms linked by acetate or benzoate ions. The type of magnetic interaction in these materials is based on their chemical, electronic, and architectural structures. Thus a detailed study is necessary to understand the macroscopic properties of these polymers.

Metal(II)−bppz complexes in the presence of halides are of particular interest, as the latter can also participate in metal−metal bridging. Only a few coordination polymers containing pyrazine or its derivatives and bridging halide ions have been structurally characterized.[9,10] Fetzer et al.[11] were able to grow single crystals of $[CuX_2(pyz)]_n$ (X = Cl, Br) by gel crystallization. However, complexes of bppz are difficult to obtain in a highly crystalline form and in most cases only insoluble powder samples were obtained. The structure solution is of particular interest, as the metal centers in such compounds can exhibit intramolecular ferromagnetic coupling.[12]

Here we present the single-crystal analysis of the binuclear complex $[Ni_2(bppz)(H_2O)_8](SO_4)_2 \cdot 2H_2O$ **(1)** and we also report the structures of $\{[Ni_2Cl_2(bppz)(H_2O)_2(CH_3OH)_2]Cl_2\}_n$ **(2)** and

[⊗] Abstract published in *Advance ACS Abstracts,* July 15, 1997.

(1) Chen, C.-T.; Suslick, K. S. *Coord. Chem. Rev.* **1993**, *128*, 293.
(2) Neels, A. Thesis, Université de Neuchâtel, Switzerland, **1995**.
(3) Serroni, S.; Denti, G. *Inorg. Chem.* **1992**, *31*, 4251.
(4) Denti, G.; Serroni, S.; Campagna, S.; Ricevuto, V.; Juris, A.; Ciano, M.; Balzani, V. *Inorg. Chim. Acta* **1992**, *198*−*200*, 507.
(5) Neels, A.; Stoeckli-Evans, H. *Chimia* **1993**, *47*, 198.
(6) Escuer, A.; Comas, T.; Vincente, R.; Ribas, J. *Transition Met. Chem.* (*London*) **1993**, *18*, 42.
(7) Neels, A.; Stoeckli-Evans, H.; Escuer, A.; Vincente, R. *Inorg. Chem.* **1995**, *34*, 1946.
(8) Neels, A.; Stoeckli-Evans, H.; Escuer, A.; Vincente, R. *Inorg. Chim. Acta* **1997,** in press.
(9) Lindroos, S.; Lumme, P. *Acta Crystallogr.* **1990**, *C46*, 2039.
(10) Munakata, M.; Kuroda-Sowa, T.; Maekawa, M.; Honda, A.; Kitagawa, S. *J. Chem. Soc., Dalton Trans.* **1994**, 2771.
(11) Fetzer, T.; Lentz, A.; Debaerdemaeker, T. *Z. Naturforsch.* **1989**, *44B*, 553.
(12) Journaux, Y.; Kahn, O. *J. Chem. Soc., Dalton Trans.* **1979**, 1575.

S0020-1669(97)00175-4 CCC: $14.00

Table 1. Crystallographic Data for Compounds **1**−**3**

	1[a]	**2**[b]	**3**[b]
empirical formula	$C_{14}H_{30}N_4Ni_2O_{18}S_2$	$C_{16}H_{22}Cl_4N_4Ni_2O_2$	$C_{14}H_{10}N_4Cu_2Cl_4$
fw	723.93	591.56	503.16
a, Å	8.372(2)	8.7014(4)	13.9124(5)
b, Å	18.301(2)	10.1465(5)	6.1844(2)
c, Å	17.197(2)	8.0303(3)	10.1572(3)
α, deg	90	116.095(2)	90
β, deg	97.54(2)	112.713(3)	112.952(3)
γ, deg	90	64.056(3)	90
V, Å^3	2611.9(9)	555.84(2)	804.74(5)
Z	4	1	2
space group	$P2_1/n$ (No. 14)	$P\bar{1}$ (No. 2)	$C2/m$ (No. 12)
T, K	163	293	293
ρ_{calc}, g cm^{-3}	1.841	1.767	2.074
λ(Cu Kα), Å	1.541 78	1.5406, 1.5444	1.5406, 1.5444
μ(Cu Kα), cm^{-1}	41.22	69.14	95.42
2θ range, deg	6−120.3	9−80	8−80
no. of reflns			
collected	4361	1794 ($K\alpha_1 + K\alpha_2$)	568 ($K\alpha_1 + K\alpha_2$)
obs	3897 ($I > 3\sigma(I)$)	($I > 1\sigma(I)$)	($I > 1\sigma(I)$)
no. of soft constraints	—	43	32
	$R_F = 0.058$[c]	$R_{wp} = 0.124$[e]	$R_{wp} = 0.054$[e]
	$R_w = 0.052$[d]	$R_p = 0.095$[f]	$R_p = 0.037$[f]
		$R_F = 0.045$[d]	$R_F = 0.063$[d]

[a] Single-crystal data. [b] Powder diffraction data. [c] $R_F = \langle||F_o| - |F_c||\rangle/\langle|F_o|\rangle$. [d] $R_w = [\sum w(|F_o| - |F_c|)^2/\sum wF_o^2]^{1/2}$. [e] $R_{wp} = [\sum w(I_o - I_c)^2/\sum wI_o^2]^{1/2}$. [f] $R_p = \sum|I_o - I_c|/\sum I_c$.

$[Cu_2Cl_4(bppz)]_n$ **(3)**, determined *ab initio* by the use of X-ray powder diffraction data. The nickel(II) complex of bppz **(2)** is a one-dimensional polymer, while the copper(II) compound **(3)** forms a new type of layer compound.

Experimental Section

Materials and Methods. All chemicals were used as received without further purification. The synthesis and analytical and spectroscopic data for the ligand bppz have been reported elsewhere.[5] Thermogravimetric analyses (TGAs) were carried out with a Du Pont Model No. 951 unit under nitrogen atmosphere between room temperature and 800 °C at a rate 10 °C/min. Infrared spectra were recorded on a Perkin-Elmer FT 1720X spectrometer using KBr pellets. Magnetic measurements were carried out on polycrystalline samples using a Qantum Design SQUID susceptometer. C, H, and N microanalyses were carried out by Galbraith Laboratories, Knoxville, TN.

Preparation of $[Ni_2(bppz)(H_2O)_8](SO_4)_2\cdot 2H_2O$ (1). 2,5-Bis(2-pyridyl)pyrazine (10 mg, 0.04 mmol) in methanol (10 mL) was added to an aqueous solution of $NiSO_4\cdot 6H_2O$ (34 mg, 0.13mmol, 5 mL) at room temperature. On slow evaporation, light green crystals were obtained after a few days (yield 10 mg, 35%). Selected IR data (cm^{-1}): 3268 ss (b), 1661 m (b), 1606 w, 1576 m, 1509 w, 1474 m, 1440 s, 1366 s, 1089 ss (b). Anal. Calcd for $C_{14}H_{30}N_4Ni_2O_{18}S_2$: C, 23.21; H, 4.14; N, 7.74. Found: C, 22.85; H, 4.44; N, 7.92.

Preparation of $\{[Ni_2Cl_2(bppz)(H_2O)_2(CH_3OH)_2]Cl_2\}_n$ (2). A solution of 2,5-bis(2-pyridyl)pyrazine (192 mg, 0.82 mmol) in methylene chloride (10 mL) was added to a solution of $NiCl_2\cdot 6H_2O$ (784 mg, 3.3 mmol) in methanol (20 mL) at room temperature. A light brown precipitate was obtained after several minutes. The product was filtered out before the total evaporation of the solvent (yield 270 mg, 56%). Selected IR data (cm^{-1}): 3309 ss (b), 1630 m (b), 1618 s, 1603 s, 1572 w, 1510 m, 1473 m, 1443 s, 1433 s, 1365 s. Anal. Calcd for $C_{16}H_{22}Cl_4N_4Ni_2O_4$: C, 32.46; H, 3.72; N, 9.47; H_2O/CH_3OH, 16.90. Found: C, 29.37; H, 4.07; N, 9.29; H_2O/CH_3OH (TGA), 18.57.

Preparation of $[Cu_2Cl_4(bppz)]_n$ (3). A solution of 2,5-bis(2-pyridyl)pyrazine (100 mg, 0.43 mmol) in tetrahydrofuran (5 mL) was added to an aqueous solution of $CuCl_2\cdot 2H_2O$ (784 mg, 3.3 mmol, 50 mL) at room temperature. The solution was filtered after standing for several hours; a green microcrystalline product was obtained after a second filtration before the total evaporation of the solvent (yield 104 mg, 32%). Selected IR data (cm^{-1}): 3067 w, 1604 s, 1568 w, 1520 m, 1508 w, 1464 s, 1437 ss, 1369 s, 1335 w. Anal. Calcd for $C_{14}H_{10}Cl_4Cu_2N_4$: C, 33.39; H, 1.99; N, 11.13. Found: C, 32.13; H, 1.84; N, 10.75.

X-ray Data Collection and Structure Solution and Refinement for Compound 1. A light green crystal having approximate dimensions of 0.30 × 0.30 × 0.20 mm was mounted on a glass fiber. All measurements were made on a Rigaku AFC5R diffractometer with graphite-monochromated Cu Kα (1.541 78 Å) radiation and a 12 kW rotating anode generator. Cell constants and an orientation matrix for data collection, obtained from a least-squares refinement of the setting angles of 25 carefully centered reflections in the range $55.65° < 2\theta < 78.51°$, corresponded to a primitive monoclinic cell. The space group was found to be $P2_1/n$ according to systematic absences. The data were collected at 163 K using the $\omega-2\theta$ scan technique to a maximum 2θ value of 120.3°. ω scans of several intense reflections, made prior to data collection, had an average width at half-height of 0.21° with a takeoff angle of 6.0°. Scans of $(1.21 + 0.30 \tan\theta)°$ were made at a speed of 16.0°/min (in ω). The weak reflections ($I < 10.0\sigma(I)$) were rescanned (maximum of three scans), and the counts were accumulated to ensure good counting statistics. Stationary-background counts were recorded on each side of the reflection. The ratio of peak counting time to background counting time was 2:1. During data collection, three representative reflections were measured after every 150 reflections. A linear coefficient was applied to the data to account for the 3.6% decay observed. An empirical absorption correction based on azimuthal scans of several reflections was applied ($T_{min} = 0.92$, $T_{max} = 1.00$). The data were corrected for Lorentz and polarization effects. The structure was solved by direct methods[13] and Fourier techniques.[14] The non-hydrogen atoms were refined anisotropically. Hydrogen atoms were included in calculated positions and held fixed. All calculations and drawings were performed using the TEXSAN crystallographic software.[15] Crystallographic data for **1** are summarized in Table 1. Positional and thermal parameters for this compound are given in Table 2, and selected bond distances and angles are listed in Table 3.

X-ray Data Collection for Compounds 2 and 3. Step-scanned X-ray powder data for both compounds were collected on the finely ground samples, side-loaded into a flat sample holder, by means of a Rigaku computer automated diffractometer. The X-ray source was a

(13) Altomare, A.; Cascarano, G.; Giacovazzo, C.; Guagliardi, A.; Burla, M. C.; Polidori, G.; Camalli, M. SIR92. *J. Appl. Crystallogr.* **1994**, *27*, 435.

(14) Beurskens, P. T.; Admiraal, G.; Beurskens, G.; Bosman, W. P.; Garcia-Granda, S.; Gould, R. O.; Smits, J. M. M.; Smykalla, C. *DIRDIF92*: *The DIRDIF program system*; Technical Report; Crystallography Laboratory, University of Nijmegen: Nijmegen, The Netherlands, 1992.

(15) TEXSAN: *Structure analysis package*, revised; Molecular Structure Corp.: The Woodlands, TX, 1987.

Table 2. Positional and Thermal Parameters for Complex **1**

	x	*y*	*z*	B_{eq}[a]
Ni1	0.85389(9)	0.28326(4)	0.01201(4)	1.16(3)
Ni2	0.62330(9)	0.49896(4)	0.30605(4)	1.16(3)
S1	0.7944(1)	0.23403(6)	0.29992(6)	1.29(4)
S2	0.8045(1)	0.36841(6)	0.58201(6)	1.24(4)
O1	0.9686(4)	0.2139(2)	−0.0563(2)	1.4(1)
O2	0.6607(4)	0.2128(2)	−0.0026(2)	2.1(1)
O3	0.9522(4)	0.2272(2)	0.1099(2)	2.1(1)
O4	0.7340(4)	0.3396(2)	−0.0822(2)	1.5(1)
O5	0.5665(4)	0.5363(2)	0.4122(2)	1.7(1)
O6	0.8107(4)	0.5679(2)	0.3044(2)	1.5(1)
O7	0.4738(4)	0.5750(2)	0.2431(2)	1.6(1)
O8	0.7739(4)	0.4280(2)	0.3755(2)	1.5(1)
O9	0.8508(4)	0.3093(2)	0.2993(2)	2.1(1)
O10	0.7557(4)	0.2083(2)	0.2174(2)	1.7(1)
O11	0.9183(4)	0.1853(2)	0.3406(2)	2.3(1)
O12	0.6464(4)	0.2298(2)	0.3371(2)	1.8(1)
O13	0.9187(4)	0.4310(2)	0.5907(2)	1.7(1)
O14	0.6713(4)	0.3877(2)	0.5201(2)	1.5(1)
O15	0.7339(4)	0.3578(2)	0.6556(2)	1.7(1)
O16	0.8849(4)	0.3017(2)	0.5620(2)	2.1(1)
O17	0.1566(4)	0.4398(2)	0.4899(2)	1.7(1)
O18	0.9140(4)	0.3731(2)	−0.1964(2)	1.9(1)
N1	0.7611(4)	0.3526(2)	0.0906(2)	1.2(1)
N2	0.6827(4)	0.4457(2)	0.2069(2)	1.3(1)
N3	1.0343(4)	0.3625(2)	0.0287(2)	1.3(2)
N4	0.4395(4)	0.4249(2)	0.2857(2)	1.3(2)
C1	0.8571(5)	0.4094(2)	0.1150(2)	1.2(2)
C2	0.8159(5)	0.4568(2)	0.1731(3)	1.3(2)
C3	0.5899(5)	0.3878(2)	0.1844(2)	1.2(2)
C4	0.6276(5)	0.3417(2)	0.1252(3)	1.4(2)
C5	1.0068(5)	0.4169(2)	0.0788(2)	1.2(2)
C6	1.1150(6)	0.4741(2)	0.0965(3)	1.7(2)
C7	1.2535(6)	0.4760(3)	0.0599(3)	1.8(2)
C8	1.2801(6)	0.4205(3)	0.0083(3)	1.9(2)
C9	1.1684(6)	0.3648(3)	−0.0051(3)	1.7(2)
C10	0.4482(5)	0.3772(2)	0.2269(3)	1.2(2)
C11	0.3349(6)	0.3232(2)	0.2080(3)	1.6(2)
C12	0.2054(6)	0.3196(3)	0.2505(3)	1.9(2)
C13	0.1935(6)	0.3695(3)	0.3093(3)	2.1(2)
C14	0.3132(6)	0.4210(3)	0.3261(3)	1.9(2)

[a] $B_{eq} = {}^8/_3\pi^2[U_{11}(aa^*)^2 + U_{22}(bb^*)^2 + U_{33}(cc^*)^2 + 2U_{12}aa^*bb^* \cos\gamma + 2U_{13}aa^*cc^* \cos\beta + 2U_{23}bb^*cc^* \cos\alpha]$.

Table 3. Selected Bond Distances (Å) and Bond Angles (deg) for Complex **1**

Ni1−O1	2.052(3)	Ni2−O5	2.063(3)
Ni1−O2	2.053(3)	Ni2−O6	2.016(3)
Ni1−O3	2.050(3)	Ni2−O7	2.079(3)
Ni1−O4	2.066(3)	Ni2−O8	2.076(3)
Ni1−N1	2.078(4)	Ni2−N2	2.079(4)
Ni1−N3	2.086(4)	Ni2−N4	2.047(4)
S−O	1.455(3)−1.485(3)		
N−C	1.332(5)−1.354(5)		
$(C-C)_{arom}$	1.375(6)−1.401(6)	Ni1−Ni2 (intra)	6.89(1)
$(C-C)_{aliph}$	1.476(6)−1.485(6)	Ni1−Ni2 (inter)	6.06(1)

O1−Ni1−O2	87.5(1)	O5−Ni2−O6	94.3(1)
O1−Ni1−O3	89.6(1)	O5−Ni2−O7	92.6(1)
O1−Ni1−O4	94.3(1)	O5−Ni2−O8	83.8(1)
O1−Ni1−N1	173.5(1)	O5−Ni2−N2	171.3(1)
O1−Ni1−N3	97.2(1)	O5−Ni2−N4	96.6(1)
O2−Ni1−O3	91.0(1)	O6−Ni2−O7	89.5(1)
O2−Ni1−O4	85.3(1)	O6−Ni2−O8	89.1(1)
O2−Ni1−N1	96.4(1)	O6−Ni2−N2	90.7(1)
O2−Ni1−N3	174.6(1)	O6−Ni2−N4	168.9(1)
O3−Ni1−O4	174.5(1)	O7−Ni2−O8	176.0(1)
O3−Ni1−N1	85.2(1)	O7−Ni2−N2	94.5(1)
O3−Ni1−N3	91.7(1)	O7−Ni2−N4	88.1(1)
O4−Ni1−N1	91.2(1)	O8−Ni2−N2	89.2(1)
O4−Ni1−N3	91.7(1)	O8−Ni2−N4	94.1(1)
N1−Ni1−N3	179.1(1)	N2−Ni2−N4	78.8(1)

rotating anode operating at 50 kV and 180 mA with a copper target and graphite-monochromated radiation. Data for compound **2** were collected between 9 and 80° in 2θ with a step size of 0.01° and a counting time of 10 s/step. For compound **3**, the same step size and counting time were used, but the 2θ range was 8−80°. Data were mathematically stripped of the $K\alpha_2$ contribution, and peak selection was conducted.[16] The powder pattern was indexed by Ito methods[17] based on the first 20 observed reflections. The best solution (FOM = 31), which indexed all the peaks of compound **2**, indicated a triclinic cell. The initial choice of the centric space group $P\bar{1}$ was found to be correct from the successful solution and refinement of the structure. The best solution (FOM = 34) for compound **3** corresponded to a monoclinic unit cell. The indexed reflections showed systematic absences consistent with the space group *C*2/*m*. Crystallographic details for compounds **2** and **3** are given in Table 1.

Structure Solution and Rietveld Refinement for Compound 2. Integrated intensities were extracted from the profile over the range 8° < 2θ < 80° by decomposition methods as described by Rudolf and Clearfield.[16] This procedure produced 49 single indexed reflections up to a 2θ limit of 55°. A Patterson map was computed using this data set in the TEXSAN series of single-crystal programs. The positions of the nickel atom and the coordinated chlorine atom were located from this Patterson map. An octahedral coordination around the metal was built on the basis of metal−metal distances and the chlorine positions. This structural model was used for the Rietveld profile refinement in GSAS.[18] After the initial refinement of the scale, background, and unit cell constants, the atomic positions were refined using soft constraints which define the expected octahedral coordination sphere of the metal within some allowable errors. The Ni−O(N) and Ni−Cl distances were held at 2.05(1) and 2.40(1) Å, respectively. The nickel octahedral geometry was obtained by constraining the N(O)−N(O), N(O)−Cl, and Cl−Cl nonbonding distances to 2.90(1), 3.15(1), and 3.40(1) Å, respectively. The carbon atoms of the bppz ligand were obtained from the difference Fourier map and by model building and were included in the refinement. The aromatic N−C and C−C bond lengths in bppz were constrained to 1.34(1) and 1.38(1) Å, while the C−C single-bond length between the aromatic rings was held at 1.47(1) Å. Final refinement was carried out against the observed powder diffraction data using soft constraints for all the atoms. The weight was reduced as the refinement progressed, but the constraints could not be removed completely without reducing the stability of the refinement. All atoms were refined isotropically. In the final cycles of refinement, the shifts in all parameters were less than their estimated standard deviations. Neutral-atom scattering factors were used for all atoms. No corrections were made for anomalous dispersion, absorption effects, or preferred orientation. A final Rietveld plot is given in Figure 1. No impurity lines could be detected in the X-ray powder diffraction pattern. Positional and thermal parameters for this compound are given in Table 4, selected bonds and angles are listed in Table 5.

Structure Solution and Rietveld Refinement for Compound 3. The decomposition over the range 8° < 2θ < 80° produced 36 single indexed reflections up to a 2θ limit of 60° in this case. A Patterson map was computed using this data set. According to the molecular formula and the unit cell volume, the metal atom has to lie on a special position. The copper atom in this complex was located on a mirror plane at (−0.2354, 0, 0.1324). In this position, one set of symmetry-related copper atoms are 6.7 Å apart, which corresponds to metals bridged by the bppz ligand. The position of one chlorine atom was derived from the Cu−Cl vector in the Patterson map. For the metal coordination including the organic ligand, a structural model was developed on the basis of the above metal−metal distances and the chlorine positions. This model was used for full pattern refinement against the observed powder diffraction data in GSAS using soft constraints as described above for compound **2**. The weight for the soft constraints was reduced as the refinement progressed, but the constraints could not be removed completely without reducing the stability of the refinement. All atoms were refined isotropically. In the final cycles of refinement, the shifts in all parameters were less than their estimated standard deviations. Neutral-atom scattering factors were used for all atoms. No corrections were made for anomalous

(16) Rudolf, P. R.; Clearfield, A. *Inorg. Chem.* **1989**, *28*, 1706.
(17) Visser, J. W. *J. Appl. Crystallogr.* **1969**, *2*, 89.
(18) Larson, A.; Von Dreele, R. B. *GSAS*: *Generalized Structure Analysis System*; Los Alamos National Laboratory: Los Alamos, NM, 1994.

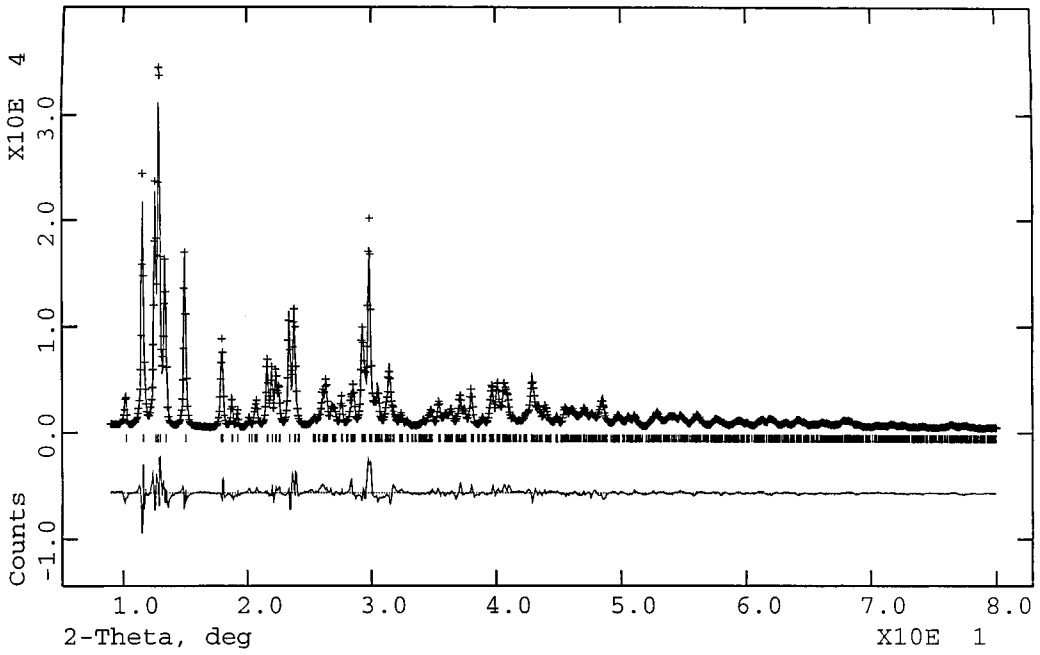

Figure 1. Observed (+) and calculated (—) profiles for the Rietveld refinement for complex **2**. The bottom curve is the difference plot on the same intensity scale.

Table 4. Positional and Thermal Parameters for Complex **2**

	x	*y*	*z*	U_{iso},[a] Å^2
Ni1	0.0065(6)	0.1961(4)	0.0745(5)	0.058(1)
Cl1	−0.0540(7)	0.0468(6)	0.1973(6)	0.046(2)
O1	−0.263(1)	0.284(1)	−0.056(2)	0.014(5)
O2	0.064(1)	0.301(1)	−0.065(1)	0.036(5)
N1	0.271(1)	0.145(2)	0.241(2)	0.014[b]
N2	−0.020(2)	0.388(1)	0.325(1)	0.014[b]
C1	0.142(2)	0.386(2)	0.452(3)	0.014[b]
C2	−0.170(2)	0.501(2)	0.374(2)	0.014[b]
C3	0.308(2)	0.257(2)	0.418(3)	0.014[b]
C4	0.480(3)	0.239(2)	0.552(2)	0.014[b]
C5	0.598(2)	0.105(2)	0.478(3)	0.014[b]
C6	0.573(2)	−0.006(2)	0.286(3)	0.014[b]
C7	0.406(3)	0.014(2)	0.169(2)	0.014[b]
C8	−0.025(3)	0.314(2)	−0.259(2)	0.088(6)
Cl2	0.3994(8)	0.3926(6)	0.0913(7)	0.048(5)

[a] $U_{iso} = B_{iso}/8\pi^2$. [b] Constrained to be equal to U_{iso} of O1.

dispersion, absorption effects, or preferred orientation. A final Rietveld difference plot is given in Figure 2. No impurity lines could be detected in the X-ray powder diffraction pattern. Positional and thermal parameters for this compound are given in Table 6, and selected bonds and angles are listed in Table 7.

Results

Thermal Analysis and Spectral Characterization of the Compounds. Thermal analysis was performed for compounds **2** and **3**, obtained in microcrystalline form, between room temperature and 800 °C. The release of the coordinated solvent molecules in the nickel coordination polymer **2** begins at about 50 °C, and the process is complete at about 170 °C. The observed weight loss of 18.57% corresponds to the release of two water and two methanol molecules per $[Ni_2Cl_4(bppz)]$ unit (calculated value: 16.9%). The difference in the observed and calculated weight losses may be due to the presence of a small amount of adsorbed solvent. The presence of adsorbed solvent would also explain the low C and N values found for the microanalyses of both **2** and **3**. The decomposition of complex **2**, including the loss of the organic component, starts at 425 °C. About 75% of the organic moiety is lost up to 600 °C, and the process continues up to 800 °C. The copper coordination polymer **3** shows no weight loss up to 300 °C, indicating that no solvent molecules are present in the structure. The decomposition of this complex starts at 300 °C, 75% of the organic component is lost up to 480 °C, and this process continues up to 800 °C.

Table 5. Selected Bond Lengths (Å) and Bond Angles (deg) for Complex **2**[a]

Ni1−Ni1[a]	3.658(9)	O−C	1.48(1)
Ni1−Ni1[b]	6.90(1)	$(C-C)_{aliph}$	1.49(1)
Ni1−Cl1	2.441(10)	N−C	1.36(1)−1.40(1)
Ni1−Cl1[a]	2.466(5)	$(C-C)_{arom}$	1.34(1)−1.46(1)
Ni1−O1	2.118(9)		
Ni1−O2	2.146(17)		
Ni1−N1	2.132(10)		
Ni1−N2	2.103(9)		
Cl1−Cl1[a]	3.271(12)		

Cl1−Ni1−Cl1[a]	83.60(24)	Cl1[a]−Ni1−N2	173.9(4)
Cl1−Ni1−O1	92.2(5)	O1−Ni1−O2	88.1(5)
Cl1−Ni1−O2	172.6(3)	O1−Ni1−N1	170.5(5)
Cl1−Ni1−N1	90.1(6)	O1−Ni1−N2	91.0(5)
Cl1−Ni1−N2	91.7(5)	O2−Ni1−N1	90.9(7)
Cl1[a]−Ni1−O1	93.0(3)	O2−Ni1−N2	95.8(6)
Cl1[a]−Ni1−O2	89.0(3)	N1−Ni1−N2	79.6(5)
Cl1[a]−Ni1−N1	96.4(4)		
C−N−C	120.6(6)−121.0(8)		
N−C−C	109(2)−125(1)		
C−C−C	110(1)−128(1)		

[a] Symmetry codes: (a) $-x, -y, -z$; (b) $-x, -y+1, -z+1$.

The infrared spectra for compounds **1**−**3** contain characteristic C−N and C−C vibration frequencies for the heteroatomatic rings of the ligand bppz. Evidence for the coordination of the ligand is provided by the shift of about 20 cm^{-1} of these absorption bands to higher frequencies (1450−1620 cm^{-1}), compared with the corresponding frequencies of the free ligand bppz (1435, 1455, 1566, 1585 cm^{-1}).[2] The presence of only five bands in this region indicates a symmetrical bis-bidentate coordination of the ligand with the transition metals. The infrared spectra of compounds **1** and **2** are almost identical ($\nu_{C-N,C-C}$: compound **1** 1606, 1567, 1509, 1474, 1444 cm^{-1}; compound **2** 1603, 1572, 1510, 1473, 1443 cm^{-1}). Broad O−H stretching bands for the water molecules in these compounds are seen between 3270 and 3300 cm^{-1}. The corresponding

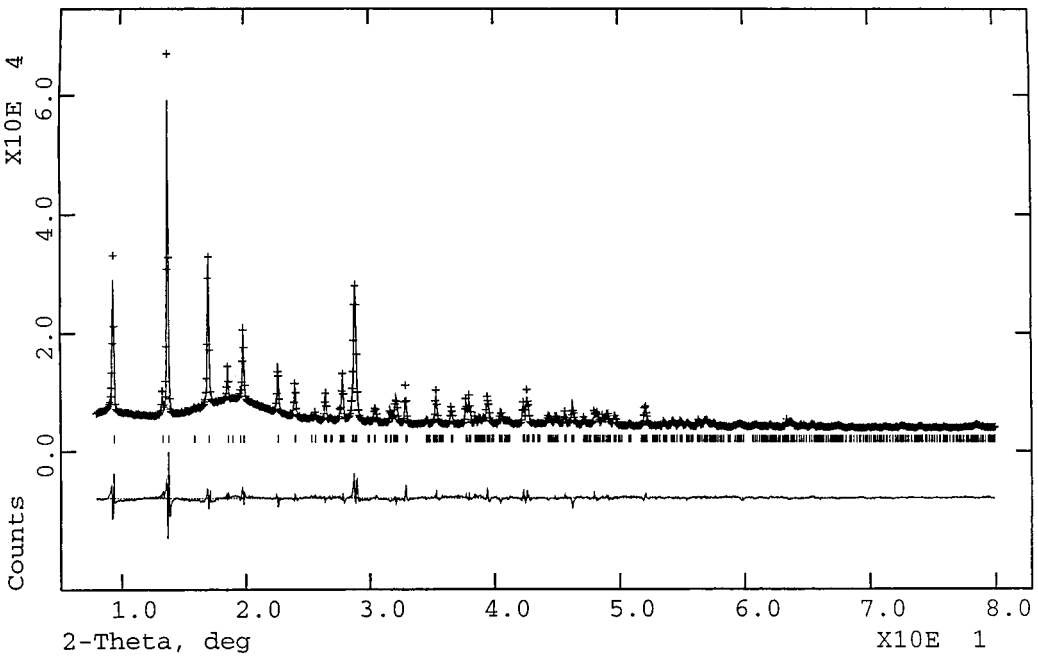

Figure 2. Observed (+) and calculated (−) profiles for the Rietveld refinement for complex **3**. The bottom curve is the difference plot on the same intensity scale.

Table 6. Positional and Thermal Parameters for Complex **3**

	x	*y*	*z*	U_{iso},[a] Å^2
Cu1	−0.2354(2)	0	0.1324(3)	0.022(1)
Cl1	−0.2223(4)	0	−0.0915(5)	0.031(2)
Cl2	−0.0549(3)	0	0.2510(4)	0.014(2)
N1	−0.3943(3)	0	0.0400(1)	0.035(6)
N2	−0.2611(8)	0	0.3167(9)	0.035[b]
C1	−0.436(1)	0	0.141(1)	0.035[b]
C2	−0.542(1)	0	0.102(1)	0.035[b]
C3	−0.365(1)	0	0.292(1)	0.035[b]
C4	−0.401(1)	0	0.399(2)	0.035[b]
C5	−0.331(1)	0	0.535(1)	0.035[b]
C6	−0.222(1)	0	0.566(1)	0.035[b]
C7	−0.189(1)	0	0.453(2)	0.035[b]

[a] $U_{iso} = B_{iso}/8\pi^2$. [b] Constrained to be equal to U_{iso} of N1.

Table 7. Selected Bond Lengths (Å) and Bond Angles (deg) for Complex **3**[a]

Cu1−Cu1[a]	6.79(1)	Cl1−Cu1−Cl1[b,c]	87.32(12)
Cu1−Cu1[b,c]	4.014(4)	Cl1−Cu1−Cl2	91.47(20)
Cu1−Cl1	2.351(7)	Cl1−Cu1−N1	91.94(16)
Cu1−Cl1[b,c]	3.1448(9)	Cl1−Cu1−N2	174.8(3)
Cu1−Cl2	2.323(4)	Cl1[b]−Cu1−Cl1[c]	159.01(14)
Cu1−N1	2.037(5)	Cl1[b,c]−Cu1−Cl2	100.21(10)
Cu1−N2	2.038(11)	Cl1[b,c]−Cu1−N1	79.96(10)
Cl1−Cu1[b,c]	3.1448(9)	Cl1[b,c]−Cu1−N2	91.75(13)
Cl1−Cl1[b,c]	3.838(7)	Cl2−Cu1−N1	176.58(21)
Cl1−Cl2	3.348(5)	Cl2−Cu1−N2	93.7(3)
		N1−Cu1−N2	82.9(3)
N−C	1.358(8)−1.374(8)	C−N−C	120.0(4)
$(C-C)_{arom}$	1.342(9)−1.389(9)	N(C)−C−C	115(1)−123(1)
$(C-C)_{aliph}$	1.464(7)		

[a] Symmetry codes: (a) $-1-x, -y, -z$; (b) $-0.5-x, -0.5-y, -z$; (c) $-x-0.5, 0.5-y, -z$.

deformation bands are found at 1660 cm^{-1} (complex **1**) and 1620 cm^{-1} (complex **2**), respectively. These bands are clearly absent for the copper complex **3**, since it does not contain any water molecules. The absorption frequency of the aromatic system is found at 3067 cm^{-1} ($\nu_{C-N,C-C}$ for compound **3**: 1604, 1568, 1520, 1508, 1464 cm^{-1}).

Structure of $[Ni_2(bppz)(H_2O)_8](SO_4)_2\cdot 2H_2O$ (1). The nickel atoms in this binuclear complex have a nearly perfect octahedral coordination geometry. Two coordination sites are occupied by nitrogen atoms (N1, N3 for Ni1; N2, N4 for Ni2) from the bridging ligand bppz while the other four sites are provided by oxygen atoms of the water molecules (O1, O2, O3, O4 for Ni1; O5, O6, O7, O8 for Ni2). The Ni−O distances are in the range 2.02−2.08 Å. These distances are similar to those found for two Ni(II) binuclear complexes of the similar ligand 2,3,5,6-tetrakis(2-pyridyl)pyrazine (tppz), where both nickel atoms are coordinated to three water molecules each (Ni−O 2.01−2.10 Å).[19] In **1**, the average Ni−N_{pyz} bond distance is slightly longer than the average Ni−N_{py} distance (2.078 compared to 2.067 Å). This trend was observed previously in Mn(II), Fe(II), and Cu(II) complexes of bppz.[5] In the nickel complexes of tppz,[19] the trend is reversed with an average Ni−N_{pyz} distance of 2.013 Å and an average Ni−N_{py} distance of 2.082 Å. In **1**, the bppz ligand bridges the two metal atoms through chelation using its nitrogen donors, as shown in Figure 3. The intramolecular Ni1···Ni2 distance is 6.89 Å, compared to 6.65 and 6.62 Å observed in the binuclear Ni(II) complexes of tppz.[19] In **1**, the

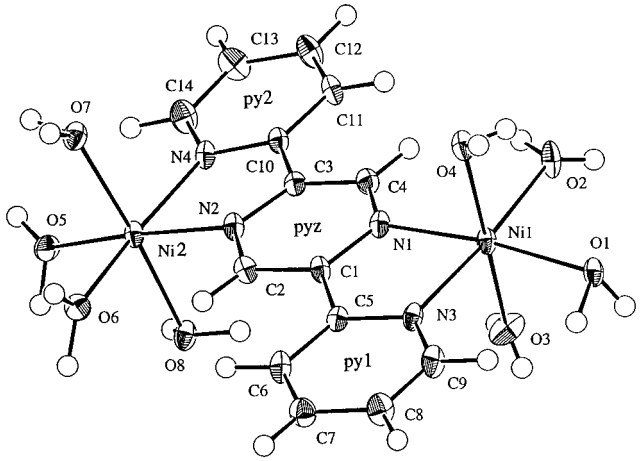

Figure 3. Structure of the $[Ni_2(bppz)(H_2O)_8]^{4+}$ cations in complex **1** showing thenumbering scheme. The hydrogen atoms are presented as small circles.

(19) Graf, M.; Stoeckli-Evans, H.; Escuer, A.; Vicente, R. *Inorg. Chim. Acta*, in press.

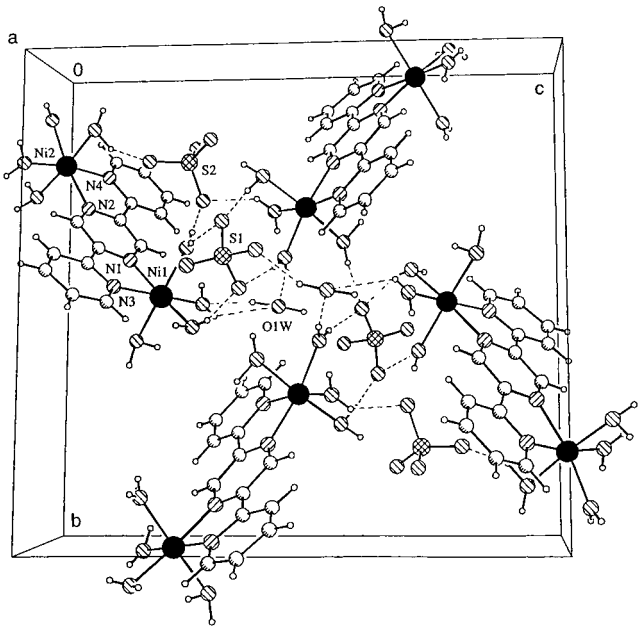

Figure 4. Arrangement of $[Ni_2(bppz)(H_2O)_8]^{4+}$ cations and sulfate anions within the unit cell. A section of the extended hydrogen-bonding network is shown by dotted lines including all fragments of structure **1**.

ligand is almost planar, with the two adjacent pyridine rings tilted by 5.5° (py1) and 3.9° (py2) with respect to the pyrazine ring. In the centrosymmetric Mn(II), Fe(II), and Cu(II) binuclear complexes of bppz,[5] the same dihedral angles were 2.6, 4.0, and 8.5°, respectively. In the crystal of **1**, the binuclear $[Ni_2(bppz)(H_2O)_8]^{4+}$ cations are linked to one other by extensive hydrogen bonds (O···O = 2.654(4)−2.892(4) Å) involving sulfate oxygens and oxygen atoms of both coordinated water molecules and the water molecules of crystallization. These interactions lead to a three-dimensional network, as shown in Figure 4. Symmetry-related molecules are well separated in such a way that no interaction between aromatic rings of different binuclear $[Ni_2(bppz)(H_2O)_8]^{4+}$ units is observed.

Structure of $\{[Ni_2Cl_2(bppz)(H_2O)_2(CH_3OH)_2]Cl_2\}_n$ (2). The structure of this complex consists of centrosymmetric $[Ni_2(bppz)]$ binuclear units linked by two chlorine atoms, forming a zigzag one-dimensional chain running along the direction [011] (Figure 5). The nickel atom is octahedrally coordinated, with two coordination sites occupied by nitrogen atoms from the bis-bidentate ligand bppz (Ni−N_{pyz} 2.132(10) Å and Ni−N_{py} 2.103(9) Å). Two bridging chloride ions (Ni−Cl1 2.441(10) and Ni−Cl1a 2.466(5) Å) and two oxygen atoms (Ni−O1 2.118(9) and Ni1-O2 2.146(17) Å) from the coordinated solvent molecules H_2O and CH_3OH, respectively, complete the octahedral coordination. The nickel coordination geometry in this compound is slightly different from that found for the binuclear complex **1**. Here the coordination geometry is slightly distorted due to the presence of the bridging chloride ions (Ni1···Ni1a 3.66(1) Å, Cl1−Ni−Cl1a 83.6(2)°, Ni1−Cl1−Ni1a 98.4(2)°). The Ni−O and Ni−N distances are slightly longer than the corresponding bond lengths in **1**. The bppz ligand is also less planar in this polymeric compound, with a dihedral angle of 8.1° between the pyrazine and pyridine rings, compared to 3.9 and 5.5° in compound **1**. The nickel···nickel intramolecular distance between metals bridged by the bppz ligand is 6.90 Å. In the crystal, the polymer chains are linked by hydrogen bonds involving the H_2O and CH_3OH molecules and noncoordinated chloride ions (Cl2···O1,O2 = 3.07(1) Å). This leads to a loosely connected two-dimensional network, as shown in Figure 5. The two-dimensional sheets are located in the *bc* plane and

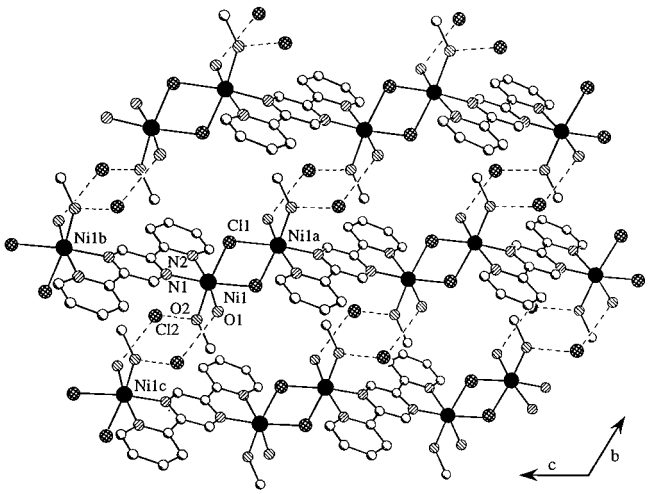

Figure 5. One-dimensional polymeric arrangement of cationic chains of $[Ni_2Cl_2(bppz)(H_2O)_2(CH_3OH)_2]_n^{2n+}$ in complex **2** viewed down the *c* axis. The hydrogen-bonding network is shown as dashed lines including coordinated and uncoordinated chlorine atoms and solvent molecules. Symmetry codes: (a) $-x, -y, -z$; (b) $-x, -y + 1, -z + 1$; (c) $-x, -y + 1, -z$.

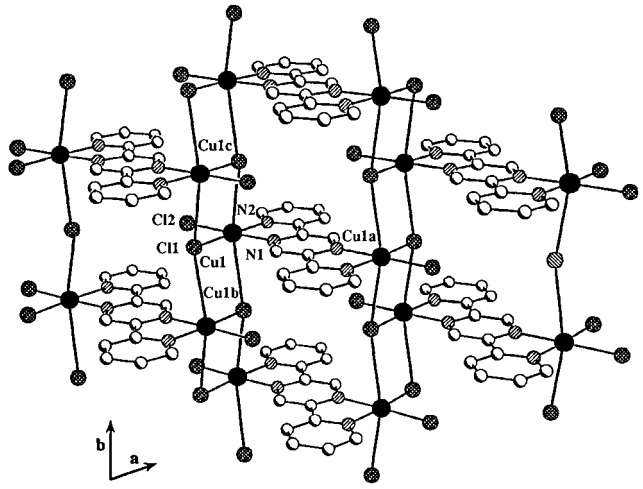

Figure 6. Two-dimensional network in complex **3**, showing the ladder type of chlorine−copper coordination and the planar bppz ligand, viewed down the *c* axis. Symmetry codes: (a) $-x - 1, -y, -z$; (b) $-0.5 - x, -0.5 - y, -z$; (c) $-0.5 - x, 0.5 - y, -z$.

separated by approximately 7.6 Å. In addition to the hydrogen bond interactions within the sheets, an end-to-end overlap of pyridine rings of neighboring planes involving C4, C5, C6, and C7 is observed (C···C = 3.40−3.55Å).

Structure of $[Cu_2Cl_4(bppz)]_n$ (3). The structure of $[Cu_2Cl_4(bppz)]_n$ consists of binuclear $[Cu_2(bppz)]$ units linked by chloride ions, forming a two-dimensional coordination polymer (Figure 6). The copper atom is coordinated by two nitrogens from the organic bridging ligand (Cu−N1 = 2.037(5) and Cu−N2 = 2.038(11) Å) and two chlorines Cl1 and Cl2 (2.351(7) and 2.323(4) Å) in the basal plane. Slightly shorter Cu−N_{pyz} and Cu−N_{py} distances were observed in the binuclear copper nitrate complex of bppz[5] (2.012 and 2.021 Å, respectively) and in two copper bppz acetate-bridged one-dimensional polymers[8] (Cu−N_{pyz} 2.024 and 2.033 Å; Cu−N_{py} 1.999 and 2.004 Å). The axial positions are occupied by symmetry-related Cl1 atoms for which the copper−chlorine distances are significantly longer (Cu−Cl1 = 3.145(1) Å) due to Jahn−Teller distortion. Thus, the coordination environment of copper is a highly distorted octahedron. All atoms in this compound are located in a mirror plane, and therefore the ligand possesses crystallographic C_s symmetry. In the binuclear copper nitrate complex of bppz,[5]

Table 8. Examples of Coordination Compounds with bppz

no.	compound	bridging unit	structure type	ref
1	$[Ni_2(bppz)(H_2O)_8](SO_4)_2 \cdot 2H_2O$	bppz	binuclear	*a*
2	$\{[Ni_2Cl_2(bppz)(H_2O)_2(CH_3OH)_2]Cl_2\}_n$	bppz and Cl^-	1D polymer	*a*
3	$[Cu_2Cl_4(bppz)]_n$	bppz and Cl^-	2D polymer	*a*
4	$[Mn_2(SCN)_4(bppz)_3(CH_3CN)_2(H_2O)_2]$	bppz	binuclear	2
5	$[Fe_2(SO_4)_2(bppz)(H_2O)_6](H_2O)_2$	bppz	binuclear	5
6	$[Cu_2(SCN)_4(bppz)(dmso)_2]$	bppz	binuclear	2
7	$[Cu_2(NO_3)_2(bppz)(H_2O)_4](NO_3)_2$	bppz	binuclear	5
8	$\{[Cu_2(OAc)_2(ClO_4)(bppz)](ClO_4)(H_2O)\}_n$	bppz and OAc^-	1D polymer	8
9	$\{[Cu_2(OBz)_3(bppz)](ClO_4)(H_2O)_2\}_n$	bppz and OBz^-	1D polymer	8
10	$[Cu_4(OAc)_8(bppz)]_n$	bppz and OAc^-	2D polymer	7

[a] This work.

the pyridine ring was twisted out of the plane of the pyrazine ring by 8.5°, while, in the two copper bppz acetate-bridged one-dimensional polymers,[8] the pyridine−pyrazine dihedral angles were 4.4 and 10.5°. In **3**, the pyrazine ring lies on an inversion center, as found for the nickel polymer in structure **2**. The bis-bidentate ligand bridges two coppers at a distance of 6.79 Å (Cu1···Cu1a), which is similar to the same distance in the binuclear copper nitrate complex (6.760 Å) of bppz[5] and the copper bppz acetate-bridged one-dimensional polymers (6.772 Å).[8] The chlorine atom Cl1 bridges three different copper atoms from three different binuclear units at a Cu1···Cu1b,c distance of 4.01 Å and a Cu1b···Cu1c distance of 6.18 Å, with a Cu1−Cl1−Cu1b,c angle equal to 92.7°. This results in the formation of a two-dimensional layer. The arrangement of copper and chloride ions leads to the formation of double chains containing four-membered rings (Cu−Cl−Cu−Cl). In the crystals of **3**, the two-dimensional sheets lie in the *ab* plane and are stacked up the *c* axes. The shortest distance between the copper atoms in this direction is 7.81 Å. The pyridine rings of molecules in neighboring sheets overlap almost perfectly at distances in the range 3.43−3.46 Å (C···C, C···N), including all atoms of the pyridine rings. The interplanar spacing is 3.09 Å with a considerable overlap of pyridine rings by interaction of their π orbitals.

Magnetic Behavior. Magnetic measurements in the range 4−300 K were performed for the nickel complexes **1** and **2**. On cooling, the $\chi_M T$ values for both compounds remain practically constant, 2.30 cm^3 K mol^{-1} for complex **1** (300−10 K) and 2.42 cm^3 K mol^{-1} (300−12 K) for complex **2**. Below 10 K (12 K for **2**), $\chi_M T$ values decay slightly (4 K: 2.01 **(1)**, 1.93 cm^3 K mol^{-1} **(2)**). This behavior is characteristic of magnetically isolated nickel(II) ions. For the binuclear complex **1**, no magnetic interaction was found between the two nickel atoms bridged by the organic ligand, which agrees with previous observations[6] made for analogous binuclear complexes containing the ligand bppz. The paramagnetic centers bridged by bppz and chloride ions in the nickel coordination polymer **2** are also magnetically isolated.

Discussion

In the formation of coordination polymers, pyrazine or its derivatives are used as bridging units between metals. We have prepared a series of 3d transition metal compounds using the bis-bidentate ligand 2,5-bis(2-pyridyl)pyrazine (bppz). The type of complex formed depends strongly on the counterions and the solvent used in such reactions as shown in Table 8 for complexes **1**−**10**.

We have characterized structurally a number of binuclear complexes containing bppz as a bridging ligand.[5] Complex formation was favored in aqueous solution in the presence of oxygen-rich anions such as nitrates and sulfates (compounds **1**, **5**, and **7**). The binuclear complex **1** is similar to the iron sulfate complex $[Fe_2(SO_4)_2(bppz)(H_2O)_6](H_2O)_2$ (**5**) described previously.[5] However, in contrast to those in the iron compound, the sulfate ions in compound **1** do not coordinate to the metal.

In order to link these binuclear M−bppz−M units into polymeric structures, counterions capable of participating in metal−metal bridging were considered. Anions such as thiocyanate (SCN^-), acetate (OAc^-), benzoate (OBz^-), and halides (Cl^-, Br^-) have been used for this purpose. The thiocyanate anions in the structures of complexes **4** and **6** act as a monodentate ligand through its nitrogen donor and do not participate in bridging. On the other hand, the use of acetate or benzoate ions resulted in the formation of polymeric species containing bppz and anion bridges between the metals (complexes **8**−**10**). Magnetic measurements[7,8] indicate antiferromagnetic properties for all three coordination polymers. Interestingly, it is found that the metal atoms bridged by the bppz ligand show a weak antiferromagnetic interaction, while strong coupling is observed between copper atoms linked by acetate or benzoate ions. Two new coordination polymers (**2**, **3**) containing chlorine atoms in bridging positions were described in this paper. The nickel complex **2** forms a one-dimensional polymer, where the metal ions are bridged by bppz and chloride ions, resulting in the formation of zigzag chains. The analogous copper compound **3** forms an extended two-dimensional polymeric structure. In this complex, the Cl1 atom bridges three different copper atoms from three different $[Cu_2Cl_4(bppz)]$ units. The arrangement of copper and chloride ions leads to the formation of double chains containing four-membered rings (Cu−Cl−Cu−Cl). This ladder type of coordination of halides to copper is known for copper(I) compounds.[9,20] In the case of $[Cu_2Cl_2(phz)]_n$ (phz = phenazine),[9] the copper−chlorine distances are in the range 2.40−2.49 Å. In compound **3**, two of the Cu−Cl bonds in the equatorial positions show similar values, but those involving the axial positions are significantly longer (3.14 Å), possibly due to the Jahn−Teller effect. The interplanar spacing of 3.36 Å found in the layers of $[Cu_2Cl_2(phz)]_n$ is larger than the spacing of 3.09 Å found in complex **3**.

Previous magnetic measurements on binuclear or polynuclear transition metal complexes have shown that no coupling between paramagnetic metal centers bridged by 2,5-bis(2-pyridyl)-pyrazine is observed[8] or that the interaction is weakly antiferromagnetic.[7] Therefore the result obtained for the binuclear nickel complex **1** is not surprising. Alternating chains (complex **2**) or two-dimensional polymers (complex **3**) are of interest in magnetic studies, as the interaction between metals bridged by bppz and the chloride ions can be studied. Studies on binuclear metal complexes containing chloride bridges indicate that, for ferromagnetic coupling between d^8 ions with an octahedral environment, the same Cl bridging atom must lie in the basal

(20) Zavalii, P. Yu.; Mys'kiv, M. G.; Gladyshevskii, E. I. *Kristallografiya* **1986**, *31*, 88.

plane of the two metal centers with a bridging angle close to 90°. This results in an accidental orthogonality of the magnetic orbitals leading to an efficient ferromagnetic exchange.[12] In the case of complexes **2** and **3**, it can be seen (Figures 5 and 6) that this situation is not achieved. Despite M−Cl−M bridging angles close to 90° (98.4 and 92.7° for **2** and **3**, respectively), two different Cl atoms lie in the different basal planes about the metal atoms. Hence, there is no overlap of the magnetic orbitals and no magnetic interaction is expected. This was confirmed by the magnetic measurements for **2,** which indicated that the paramagnetic centers are magnetically isolated. On the basis of the same reasoning, it was considered unnecessary to carry out magnetic measurements for complex **3**.

Acknowledgment. We are grateful to Prof. Albert Escuer and Prof. Ramon Vicente for the results of the magnetic measurements and very useful discussions. We wish to thank the Swiss National Science Foundation for financial support in the form of a research grant for A.N.

Supporting Information Available: Tables of anisotropic thermal parameters, hydrogen positions and *B*(eq) values, full bond lengths and angles, hydrogen bond parameters, and least-squares planes for **1**, TGA curves for **2** and **3**, IR spectra for **1**−**3**, and a figure showing the one-dimensional polymeric arrangement of the cationic chains of **2** (11 pages). Ordering information is given on any current masthead page.

IC970175I